Optimization with a Genetic Algorithm for Multilayer Electromagnetic Wave Absorption Cement Mortar Filled with Expended Perlite

Chao Ma[1], Zihao Wu[1], Shuai Xie[1,*], Xin Yang[2], Tiantian Si[1], Junyu Wu[1], Zhijiang Ji[1,*], Jing Wang[1] and Chunhong Guo[1]

[1]*State Key Laboratory of Green Building Materials, China Building Materials Academy Co., Ltd., Beijing 100024, People's Republic of China*

[2]*MCC Testing Certification Co., Ltd., Beijing 100088, People's Republic of China*

Abstract: Due to the complexity of the design of multilayer electromagnetic (EM) wave absorbing materials, it is difficult to establish the relationship between material parameters (type and filling ratios) and EM properties using traditional trial and error methods. Based on the measured EM parameters within a few materials and Boltzmann mixing theory, a database of EM parameters was thereafter built up. In this study, the genetic algorithm (GA) was used to design the multilayer wave-absorbing cement mortar. In order to verify this method, a multilayer mortar was fabricated and measured. The simulated and measured results are well consistent, which convincingly verifies computer-aided design. In addition, the optimized result expresses that the first layer as a matching layer guides EM waves into the interior of the material, while the other layers as absorption layers attenuate EM waves. The multilayer material may not meet the impedance gradient principle but still exhibits better EM wave absorption performance. The reflection loss (RL) of all optimized three layer sample is below –6.89 dB in the full frequency band and the minimum RL is –26.21 dB. This composite absorbing material and the GA method provide more design ideas for the design of future cement-based wave-absorbing materials and save a lot of time and material cost.

Keywords: Multilayer design, Genetic algorithm, Absorbing mortar, Electromagnetic wave absorption, Boltzmann, Reflection loss.

1. INTRODUCTION

Electromagnetic (EM) radiation pollution has been shown to have adverse physiological effects and the EM interference problem has exposed more hidden dangers to today's information security [1-3]. EM wave absorbing materials, which have a high efficiency of electromagnetic energy loss, are applied to prevent EM radiation, and overcome the EM pollution [4-6]. Therefore, it is of great significance to design high-performance EM wave absorbing materials. The EM wave loss function depends heavily on the absorbent agent which dispersed in the matrix. Specifically, changes in the type and content of the absorbent agent can lead to changed loss performance of EM wave absorbing material. Hence, the type and content of absorbent agent are important factors in designing EM wave absorbing materials.

Considering the fact that combination of different material and thickness can exhibit different loss capabilities. Thus, the two factor are taken into consideration in material design, and the reflection loss, input wave impedance, intrinsic impedance of each layer, frequency ranges and thickness of each layer are used to describe the EM wave-absorbing performance. Computer aided technology can establish a database of materials and thicknesses and select the optimal ratio results from them. According to some literature, genetic algorithms (GA) [7-9], particle swarm optimization (PSO) [10-12], imitation based optimization (ISO) [13], winning particle optimization (WPO) [14], artificial bee colony (ABC) algorithm [15], etc. have been used to solve EM design problems [16]. To the best of our knowledge, computer aided optimization techniques are commonly used in the design of organic matrix absorbing materials such as paraffin [8], epoxy-resin [1], thermoplastic polyurethane [17], etc. Guan *et al*. [8] optimizes the design of Co/FeSi coatings via using GA, and the optimized coating with the thickness of 2.06 mm contained 13.5% Co and 55.6% of FeSi particle. The PSO is used by Micheli *et al*. [12] to design and optimize multilayered resin absorbers contained MWCNTs and the obtained effective absorption bandwidth (EAB, RL<-20 dB) is about 10 GHz under an oblique incident condition in 2-18 GHz. Cheraghi *et al*. [13] gather the EM parameters of 109 materials from different sources and the ISO was used to design an optimized tool for the best layer wave absorber, which can be used in various

*Address correspondence to this author at the State Key Laboratory of Green Building Materials, China Building Materials Academy Co., Ltd., Beijing 100024, People's Republic of China;
E-mail: xs5649@163.com; jzj1618@126.com

E-ISSN: 2410-4701/23

applications. Yildizel *et al*. [15] designed a multi-layer microwave absorbing foam concrete (NMAFC) using ABC algorithm and the 4-layer MMAFC with 34.74 mm total thickness excessively satisfies the minimum requirement of 90% absorption in X band. However, due to the limitation of the thickness of cement-based materials, the complexity of their composition, and the randomness of their preparation, there are difficulties in designing cement-based EM wave absorbing materials. Thus, computer-aided technology is rarely applied to the design of cement-based EM wave absorbing materials.

Genetic algorithm (GA), as a classical algorithm, can obtain a global optimal solution in a database and indeed be utilized for the optimization design of EM wave absorbing material, which can save immense amounts of time and material cost. In this study, the electromagnetic parameters of cement mortar are tested, and the material database is built using Boltzmann theory. In order to obtain an efficient broadband EM wave absorption structure, the maximum RL is taken as the objective function of genetic optimization algorithm. The optimization results of double layer and three layer wave absorbing materials are presented. Comparison of experimental and calculated RL of optimized structural samples verifies the correctness of the optimization process.

2. EXPERIMENTAL AND MODELING

2.1. Experimental

P.O 42.5 R Portland cement, standard sand with particle size of 0.08 mm to 2 mm, expanded perlite (EP) with the average particle size of 0.5 mm to 1 mm and waste iron power (WIP) with average particle of size 26.833 μm were used for experimental in the current study. These raw particles were purchased from China Building Materials Academy, Xiamen ISO Standard Sand Co., Ltd., Shanghai LongYuan Industrial Co., Ltd., and Lingshou County Nonstop Mineral Products Business Department, China, respectively. The specimens were prepared by mixing mortar, WIP, EP, or carbon black (CB, Tianjin Jinqiushi Chemical Industry Co., Ltd., China) mixture with the paraffin to set ratios as list in Table **1**. The chemical compositions and basal properties of cement are listed in Table **2** and Table **3**, respectively. Table **4** lists the physical properties of CB. Dispersing agent (WinSperse 4080A, produced by Weifang Winbos New Material Co., Ltd, China.) and tap water are needed as well.

The WIP-containing mortar with or without CB were grinded into power and compressed into toroidal shaped with paraffin as binder ($\varphi_{out} = 7\ mm$, $\varphi_{in} = 3.04\ mm$ and about 3 mm thickness) and the mixture and solid paraffin had a

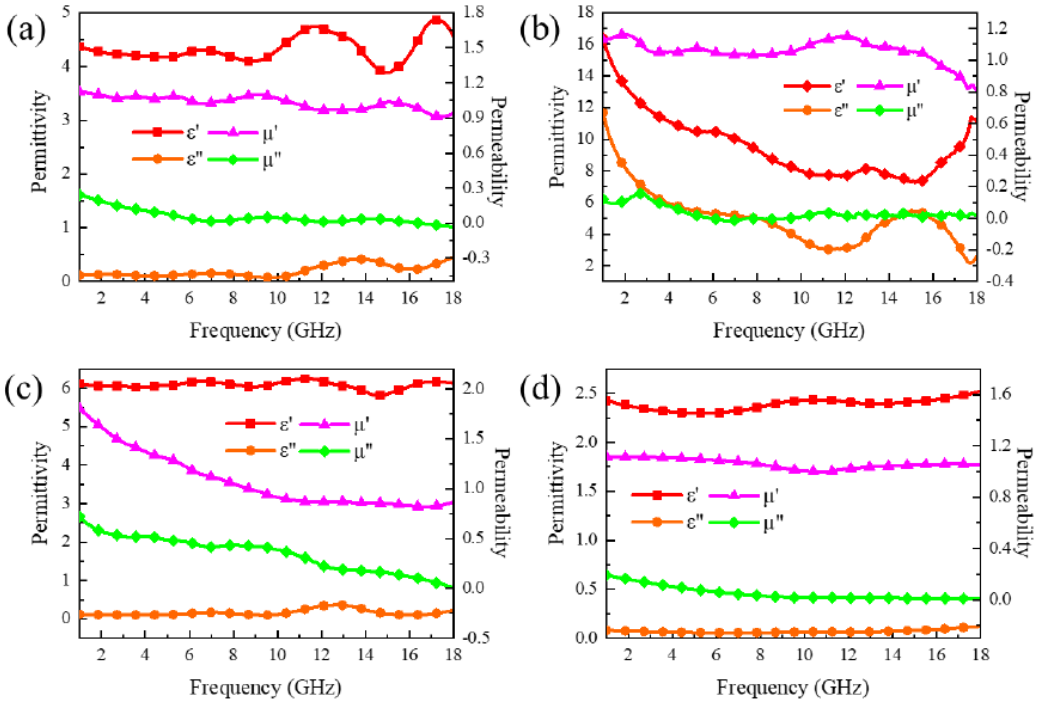

Figure 1: The EM parameters of cement (**a**), CB (**b**), WIP (**c**) and EP (**d**).

Table 1: The Specimens Prepared by Mixing Set Ratios of WIP or EP Mixture in the Paraffin Matrix

Raw material	Ratio
Mortar	Cement: Sand: Water=1:1.5:0.33
WIP/volume replacement ratio of sand	0%, 10%, 30%, 50%, 70%
EP/volume replacement ratio of mortar	0%, 20%, 25%, 30%, 35%, 40%, 45%, 50%
CB/weight ratio of cement	With or without 2%

Table 2: Cement Chemical Compositions

Component	SiO_2	Al_2O_3	Fe_2O_3	CaO	SO_3	Na_2Oeq	f-CaO	Loss	CL^-
Content (%)	20.53	4.45	3.17	62.05	2.81	0.55	0.80	1.74	0.032

Table 3: Basal Properties of Cement

Density (g/cm^3)	Specific surface area (m^2/kg)	Initial setting time (min)	Final setting time (min)	Flexural Strength (MPa)		Compressive strength (MPa)	
				3d	7d	3d	7d
3.12	359	110	171	6.0	7.5	28.0	37.9

Table 4: The Physical Properties of CB

DBP (ml/100g)	Resistivity (Ω•cm)	Particle size (nm)	Ignition loss	Ash content	Iodine adsorption number (g/kg)	pH	BET specific surface (m^2/g)	Apparent density (g/cm^3)
≥260	2.1	30-50	≤0.3%	≤0.2%	≥280	6-8	66.3	0.2～0.3
*DBP: Absorption value of dibutyl phthalate.								

mass ratio of 7:3. The complex permittivity and complex permeability were measured by coaxial transmission/reflection method on a vector network analyzer (VNA, Agilent N5234A) in 1–18 GHz. Three specimens were prepared and measured to eliminate the random error. Figure **1** shows the EM parameters of cement, CB, WIP and EP, which indicates that cement and EP have almost no loss capacity, while CB and WIP have good dielectric and magnetic loss properties, respectively [18].

2.2. The Design of Multi-Layer Absorbing Material

Generally speaking, it is difficult to achieve a perfect combination of impedance matching and maximum attenuation for single layer EM wave absorbing materials. However, multilayer materials have attracted much attention due to their simple preparation and significant results, which can broaden the EM wave absorption bandwidth. The structural schematic diagram and equivalent circuit of a multi-layer EM wave absorbing material is shown in Figure **2**. It is assumed that the last layer (the layer n+1) is an ideal conductor layer, and the first layer (the layer *1*) is in contact with air. μ_{ri} ($\mu_{ri}=\mu_{ri}^{'}-\mu_{ri}^{''}$), ε_{ri} ($\varepsilon_{ri}=\varepsilon_{ri}^{'}-\varepsilon_{ri}^{''}$) and d_i represents the complex relative permeability, complex relative permittivity, and thickness of the medium *i*, respectively. Z_{Ii} and Z_i is the input wave impedance and characteristic impedance of layer *i*, respectively, where Z_{I1} is the input impedance of the surface layer. Based on the transmission line principle [15, 19-21], when EM waves are incident perpendicular to the upper surface, the input wave impedance of each layer is as follows [17, 22].

$$Z_{I(n+1)}=0 \tag{1-1}$$

$$Z_{In}=Z_n\tanh(jk_nd_n) \tag{1-2}$$

$$Z_{Ii}=Z_i\frac{Z_{I(i+1)}+Z_i\tanh(jk_id_i)}{Z_i+Z_{I(i+1)}\tanh(jk_id_i)} \tag{1-3}$$

$$k_i=\omega\sqrt{\mu_0\mu_{ri}\varepsilon_0\varepsilon_{ri}} \tag{1-4}$$

$$Z_i=Z_0\sqrt{\frac{\mu_{ri}}{\varepsilon_{ri}}} \tag{1-5}$$

Where Z_0 ($Z_0 = \sqrt{\frac{\mu_0}{\varepsilon_0}} = 377$ Ω), μ_0 and ε_0 are the wave impedance, permeability and permittivity of free space, respectively. $\omega = 2\pi f$ is the angular frequency of the incident wave. k_i is the wave number of EMW propagation and *j* is the imaginary unit.

The EMW absorbing performance is commonly described in terms of reflection loss (RL) [23, 24]. Since the RL is a function of Z_{I1}, it can be calculated by formula (2). The RL value is smaller than -5 dB, -7 dB, -10 dB and -20 dB which indicates that 68%, 80%, 90% and 99% of EM energy is effectively dissipated, respectively.

$$RL(dB) = 20\lg\left|\frac{Z_{I1} - Z_0}{Z_{I1} + Z_0}\right| \quad (2)$$

2.3. The Genetic Algorithm Model

Genetic algorithm is a classic optimization algorithm that inspired by the principle of gene combination in biological evolution during the optimization process [8]. Generally, all free variables are placed in a vector X to form a chromosome. Each variable is considered a gene fragment, and the possible value of each chromosome represents an individual. The set of selectable chromosomes is called the population, and its number is called the population size. The initial chromosomes of the genetic algorithm are generated globally at random, and the chromosomes can be well selected for better offspring through selection, crossover, and mutation. The genetic expression corresponds to a fitness function, that is, an objective function. The genetic algorithm searches for the global minimum value of objective function to obtain the optimal solution. The flow of genetic algorithm is shown in Figure **3**.

Multilayer EM wave absorbing materials are composed of different materials, and the thickness of each layer is different. Since the impedance is related to *k* and *d*, k_n and d_n are used to represent the material and corresponding thickness of the layer *n*, respectively, so that the EM wave absorbing material can be represented by a string of variables with a length of *2n*. The relevant parameters in the genetic algorithm are as follows, the population size is 40, the generations are 300, the optimization accuracy *tolfun* is 1e-10 and the remaining parameters are system default, which is set through the *optimoptions* function. The genetic algorithm is written in MATLAB and solved using built-in *ga* functions. The conditions for the termination of the algorithm are that the optimal objective function does not change for a certain

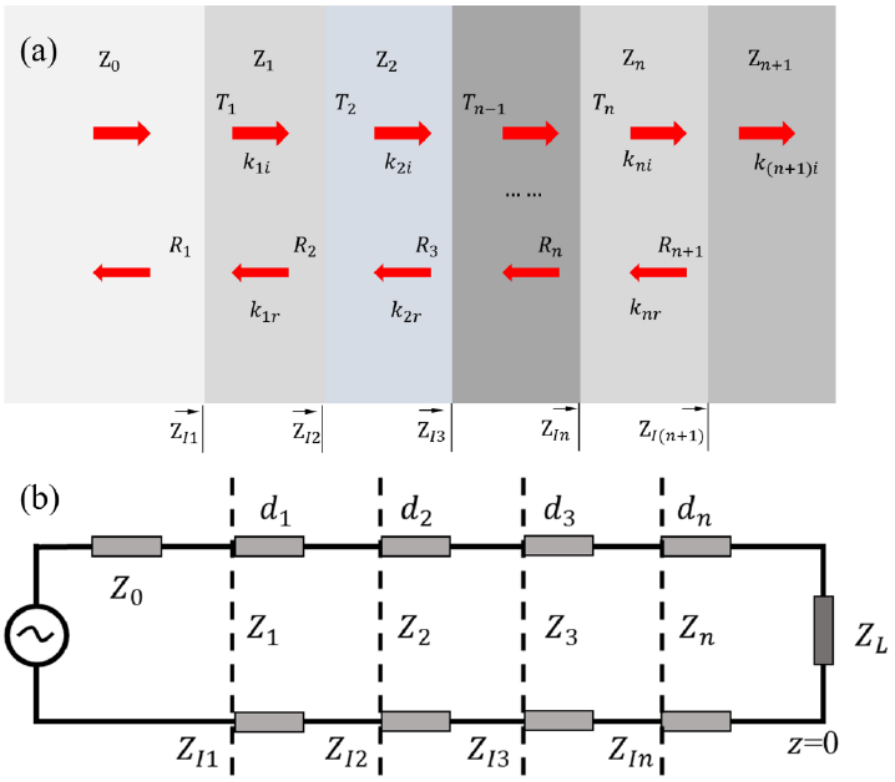

Figure 2: The structural schematic diagram (**a**) and equivalent circuit (**b**) of a multi-layer EM wave absorbing material.

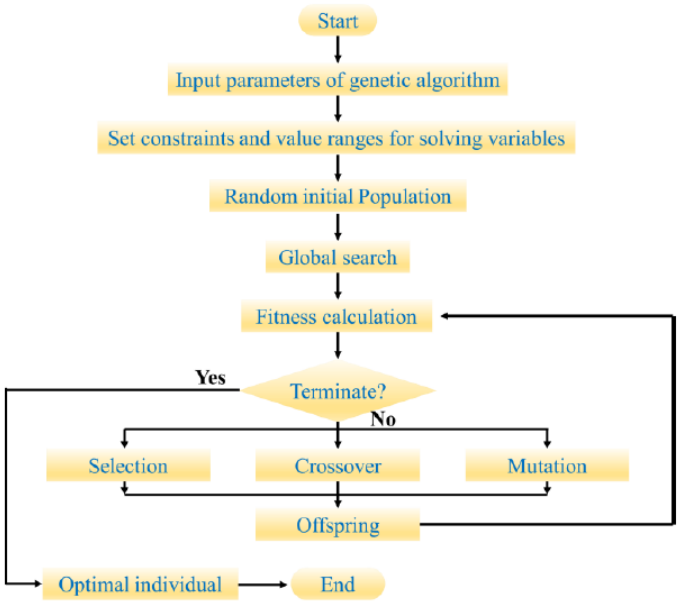

Figure 3: The flow of the genetic algorithm.

number of iterations, or the number of iterations exceeds the set value. The smaller the RL, the better the EM wave absorption ability. Therefore, in order to obtain the maximum attenuation, the following objective function (OF) based on the RL is utilized. During the OF is minimized, the layer's material and thickness should be determined.

$$\mathrm{OF} = \max(\mathrm{RL}) \tag{3}$$

3. RESULTS AND ANALYSIS

3.1. Material Library Data

EM parameters are the most important data in the calculation of EM wave absorbing materials. The polarization or magnetization vector of the medium lags behind the external alternating EM field due to damping of electric moment and magnetic moment, resulting in energy loss. Figure **4** shows the frequency dependence of EM parameters for paraffin wax composites containing mortar filled WIP. The real and imaginary part indicate the storage ability and dissipation ability of the EM energy, respectively [25, 26]. The ε' of mortar improves significantly with the addition of CB and different content of WIP, which is aligned with the Boltzmann effective medium theory (Eq.4) [27-30]. However, the $\tan\delta_e$ is insensitive to the WIP content but sensitive to CB, which indicates that CB is beneficial to increase the conductivity loss of the absorbing material. As shown in Figure **8**(**a**, **b**), the ε_r' values remain constant in the range of 1-18 GHz. Besides, the ε_r'' resonance peak is observed, which is the resonance of interfacial polarization resulting from the discrete conductive particles separated by higher-resistivity particle boundaries [31]. For the WIP-filled mortars, interfacial polarization and exchange coupling resulted from the moving charge with alternating electrical field is an important polarization mechanism [8, 32].

$$\sum_{j=1}^{N} f_j \frac{\varepsilon_j - \varepsilon_{eff}}{\varepsilon_j + 2\varepsilon_{eff}} = 0 \tag{4}$$

Where f_j is the volume fraction of each phase, ε_j, ε_{eff} are the dielectric constants of each phase and their mixtures respectively.

With the increased contents of WIP, the μ_r' increases in the range of 1-8 GHz and decreases in the range 8-18 GHz (Figure **4**(**d**)). On the whole, the variation in μ_r' is close to 1 in 8-18 GHz, which indicates that the composites possess relatively poor magnetic storage abilities in the high-frequency range [33]. At about 9 GHz, the main magnetization mechanism of the mortar filled iron powder material changes, which is from paramagnetism to diamagnetism (Figure **4**(**d**)). The realignment of molecular intrinsic magnetic moment along the external EM field is the main magnetization mode below 9 GHz. On the contrary, the rotation of electronic magnetic moment taking the direction of the magnetic field as the axis is the main magnetization mode above 9 GHz [34]. The μ_r'' values for all samples decline with increase of test frequency, so are the $\tan\delta_m$ of all samples. However, the μ_r'' values and tan*δm* enhance with the

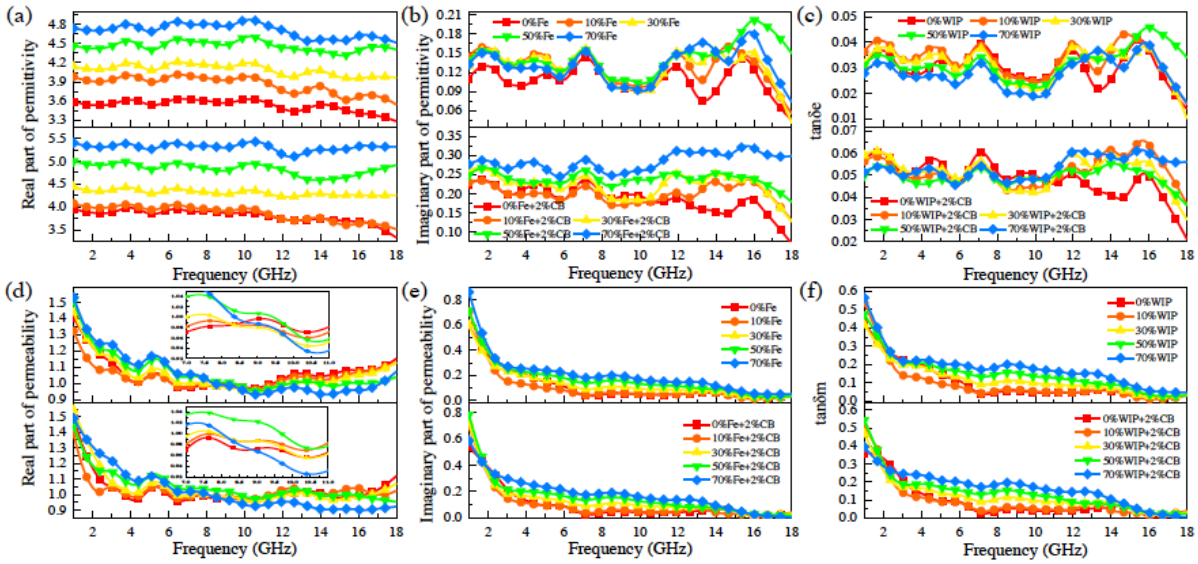

Figure 4: Frequency dependence of EM parameters for mortar/paraffin composites without EP (Data identification is unified). (**a**, **b**) complex permittivity, (**c**) Dielectric loss tangent, (**d**, **e**) Complex permeability, (**f**) Magnetic loss tangent.

increased contents of iron power, and the CB cannot enhance the magnetic loss, which indicates that the magnetic loss is an inherent property of WIP which is amplified with the increase of WIP content.

Based on Boltzmann theory (Eq.4), the EM parameters for different EP volume contents are obtained. Figure **5** shows the EM parameter of pure cement mortar (0%WIP) with different EP content. It can be seen that the dielectric constant gradually decreases, while the magnetic permeability and the loss angle tangent hardly changes with the increase of EP content, which indicates EP is a good wave transmitting material that hardly loses EM waves. The same is true for the variation of EM parameters of other matrix materials with EP content (shown in Figure **S1**-**S9**). Table **5** shows the optimization database of EM wave absorbing materials. In the genetic algorithm, the input parameter of the function is the material number, and the return variable is the EM parameter corresponding to the material. In summary, the EM parameters of all materials are shown in Figure **4**, Figure **5**, and Figure **S1**-**S9**.

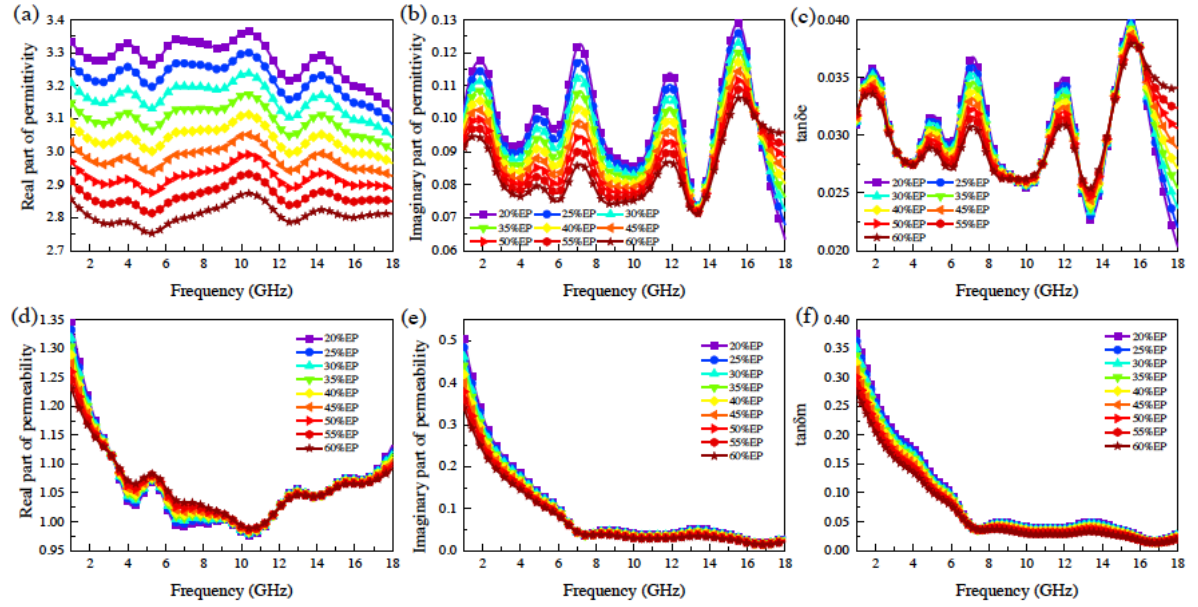

Figure 5: Frequency dependence of EM parameters for mortar (0%WIP)/paraffin composites with different EP content (Data identification is unified).

Table 5: The Optimization Database for Absorbing Materials

EP / Matrix	EP / volume ratio of mortar									
	0%	20%	25%	30%	35%	40%	45%	50%	55%	60%
0%WIP	1	2	3	4	5	6	7	8	9	10
10%WIP	11	12	13	14	15	16	17	18	19	20
30%WIP	21	22	23	24	25	26	27	28	29	30
50%WIP	31	32	33	34	35	36	37	38	39	40
70%WIP	41	42	43	44	45	46	47	48	49	50
0%WIP+2%CB	51	52	53	54	55	56	57	58	59	60
10%WIP+2%CB	61	62	63	64	65	66	67	68	69	70
30%WIP+2%CB	71	72	73	74	75	76	77	78	79	80
50%WIP+2%CB	81	82	83	84	85	86	87	88	89	90
70%WIP+2%CB	91	92	93	94	95	96	97	98	99	100
The number represents the material number.										

3.2. The RL of Multilayer EM Wave Absorption Material

Figure **6** illustrates the RL of single layer EM wave absorption material with a 20 mm thickness in the frequency ranges of 1-18 GHz, from which it can be observed that there are several evident peaks appearing in the RL curve of each specimen. The frequency at evident peaks shifts to low frequency with the increase of CB and WIP content and reduction of EP content, which can be explained by Eq.5 [35, 36]. Due to the enhancement of the EM parameter according to the Figure **4**, Figure **5**, and Figure **S1**-**S9**, the matching frequency reduces. The RL curve gradually moves downward as WIP and CB increase, indicating that the EM wave loss performance enhances (shown in Figure **6**(**a**)). However, the EM wave loss performance reduces with the increase of EP (shown in Figure **6**(**b**) and Figure **S10**), which is because an increase in EP content means a decrease in the loss medium. Interestingly, although the average RL for samples with high WIP content has increased with the increase of EP content, the RL at a specific frequency point has decreased sharply (in Figure **S10**), which expresses that the addition of EP will increase the destructive interference loss. Therefore, it can be speculated that there is strong reflection and scattering between adjacent EP particles, and destructive interference will occur when the phase difference between the two EM waves is half a wavelength. In summary, reasonable regulate the content of WIP, CB, and EP content can significantly improve the EM wave absorption ability of mortar.

$$f_m = \frac{c}{4d\sqrt{\mu_r \varepsilon_r}}(2n+1), n = 0,1,2,\cdots \tag{5}$$

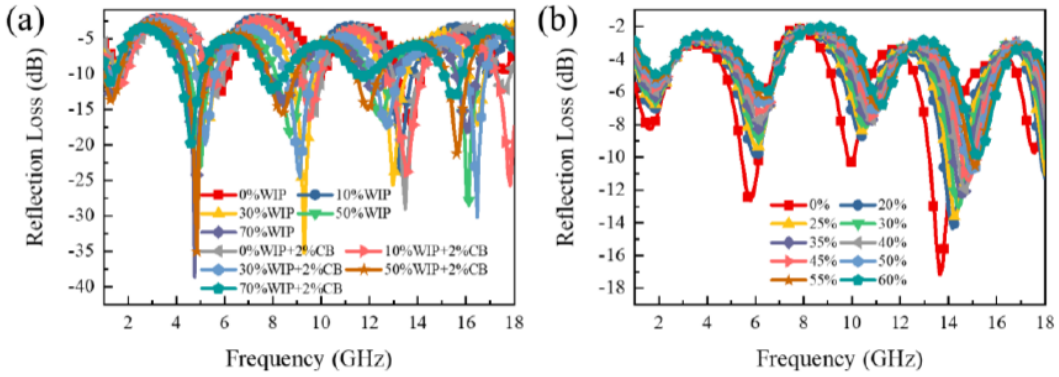

Figure 6: The RL of single layer EM wave absorption material with a 20 mm thickness. (**a**) The mortar with different WIP and CB, (**b**) the mortar containing 0%WIP with different volume content of EP.

Where f_m, *c* and *d* are the matching frequency (Hz), the velocity of light (3×10^8 m/s), and the sample thickness (m), respectively.

Genetic algorithm is used to optimize the design of double layer EM wave absorbing materials to achieve broadband absorption of 1-18 GHz. The number of corresponding free variables is 4 in the calculation process. The total design thickness does not exceed 40 mm and the average thickness of each layer is less than 20 mm. Thus, the value range of the thickness variable is [0 20], and the value range of the material variable is [1 100]. Genetic algorithms have randomness in the selection of initial populations, so each time genetic algorithms are run, the results obtained vary, but they are still the optimized results. The optimization results of the double layer material after running five times are filled in Table **6** and the RL is shown in Figure **7**. It can be found from the material composition that the first layer of material has a high content of EP and a low content of WIP and CB, and the second layer of material contains a high content of WIP, which indicates that the first layer should have a good impedance match, which can guide EM waves into the interior of the material as much as possible, and the second layer with high loss ability is the key to attenuating EM wave [6]. Thus, this combination of the matching layer (first layer) and the absorption layer (second layer) greatly improves the EM wave absorption ability of the material (The RL of all single layer material with a 40 mm thickness is shown in Figure **S11** and Figure **S12**). The RL of optimal sample D2# is less than -5.96 dB in the full frequency band, with a minimum value of -31.69 dB and an average value of -11.02 dB. Moreover, the effective absorption bandwidth (EAB, RL< -7 dB) is 15.6 GHz (1-1.3 GHz, 2-3.6 GHz, 4.1-17.8 GHz).

The optimization results of the three layer material after running five times are filled in Table **7** and the RL is shown in Figure **8**. The total design thickness does not exceed 60 mm and the average thickness of each layer is less than 20 mm. Thus, the value range of the thickness variable is [0 20], and the value range of the

Table 6: Optimization Results for Double Layer Materials

Samples		First	Second	d_total/mm	RL_{max}/dB	RL_{min}/dB	RL_{mean}/dB
D1#	Num.	3	91	37.7607	-5.8612	-23.2742	-10.7350
	d/mm	18.4542	19.3065				
D2#	Num.	6	41	37.5034	-5.9679	-31.6937	-11.0212
	d/mm	18.0808	19.4226				
D3#	Num.	18	41	39.4161	-5.6102	-31.1257	-10.9316
	d/mm	19.6412	19.7749				
D4#	Num.	2	91	38.2159	-5.8839	-25.0700	-10.6480
	d/mm	18.7684	19.4475				
D5#	Num.	4	41	37.581	-6.0018	-25.5877	-10.7844
	d/mm	18.0794	19.5016				

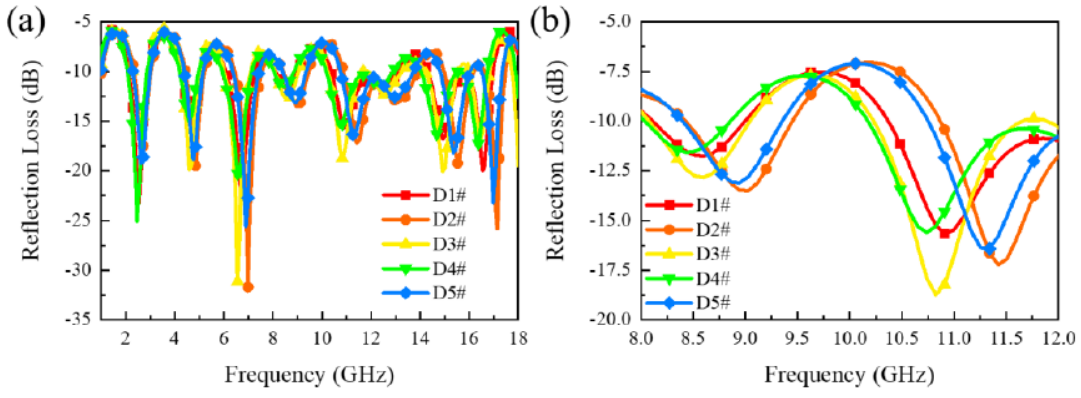

Figure 7: The RL of double layer materials.

Table 7: Optimization Results for Three Layer Materials

Samples		First	Second	Third	d_total/mm	RL_{max}/dB	RL_{min}/dB	RL_{mean}/dB
T1#	Num.	71	31	41	58.5670	-7.3622	-17.0857	-9.3681
	d/mm	19.5597	19.5083	19.499				
T2#	Num.	72	42	41	57.1936	-7.2656	-19.5659	-9.9925
	d/mm	18.1538	19.6845	19.3553				
T3#	Num.	73	81	42	56.3764	-6.9870	-26.2059	-10.2242
	d/mm	19.1429	17.9172	19.3163				
T4#	Num.	72	81	43	56.4737	-6.9293	-24.3910	-10.0158
	d/mm	17.4632	19.6275	19.383				
T5#	Num.	77	35	41	54.5159	-6.8927	-25.9410	-10.9296
	d/mm	15.5151	19.5028	19.498				

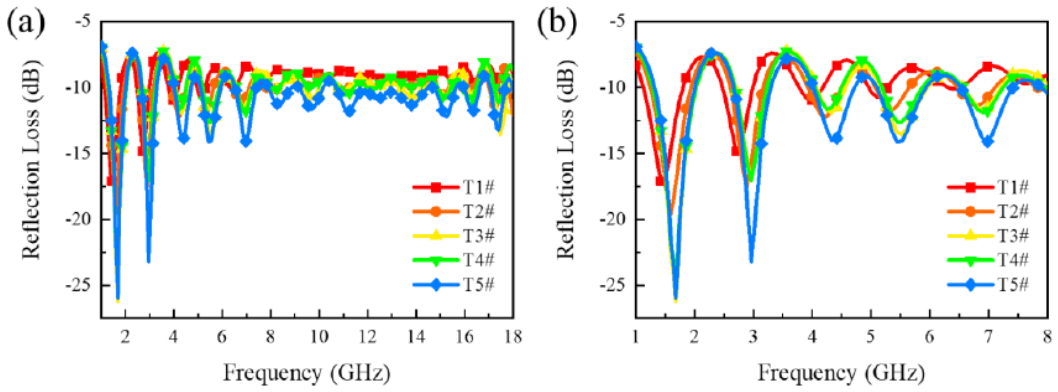

Figure 8: The RL of three layer materials.

material variable is [1 100]. Obviously, the first layer of material still contains a high EP content, providing a good impedance matching condition for the entry of EM waves. However, the second and third layers, as absorption layers, may not meet the impedance gradient principle, which increases the complexity of the design of absorbing materials. Therefore, although the impedance gradient principle, which is a universal design principle, can guide the design of multilayer materials [37, 38], there are still certain drawbacks. Computer aided optimization design is a good way to design multilayer wave absorbing materials. For example, the RL of sample T1# is below –7.36 dB in the full frequency band and a minimum RL of –26.21 dB appears in sample T3#. The lowest average RL is –10.9 dB which occurs at T5#. Although the RL varies, all the optimized sample has a RL below –6.89 dB, which indicates that the optimized sample has good EM wave loss ability, especially for low frequency improvement (by comparing Figure **8** and Figure **S13**, **S14**).

3.3. Experimental Verification

Figure **9**(**a**) shows the RL calculation result of sample T5 # and its corresponding input wave impedance of each layer. It can be found that impedance matching is only for the surface layer, while the input impedances of the other two layers do not represent the input conditions of EM waves. Therefore, the first layer is generally considered as matching layer of EM wave for multilayer absorbing materials, which can guide EM waves into the absorbing material as much as possible, so its intrinsic impedance should be as close to the air impedance as possible. As shown in Figure **9**(**b**), the intrinsic impedance of each layer's material decreases layer by layer, meeting the principle of impedance gradient, which can increase the absorption ability. Similarly, for sample T3#, the intrinsic impedance of the first layer is still closest to that of air, meeting the impedance matching, while the intrinsic impedance of the second layer material is lower than that of the third layer material, which do not meet the impedance gradient principle but still exhibits better EM wave absorption performance. Therefore, an

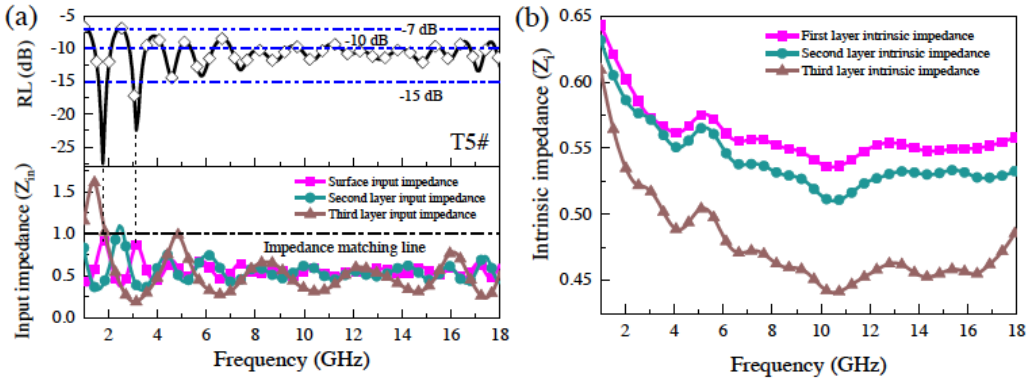

Figure 9: The impedance matching (**a**) and intrinsic impedance (**b**) of sample T5#.

excellent matching layer can increase the chances of EM waves entering the absorbing material. However, the impedance characteristics of material in other layers (collectively referred to as the absorbing layer) are no longer strictly regulated, but ultimately, the EM waves can be attenuated to the maximum extent. This undoubtedly increases the complexity of the design of absorbing materials. Thus, the application of computer aided technology greatly reduces the difficulty of designing absorbing materials and can simplify complex EM design problems.

The experimental sample (T5#) is prepared layer by layer from the third layer to the first layer. The uniformly dispersed CB solution is added to the cement and WIP mixture that is uniformly mixed according to the predetermined proportion. The mixture is quickly stirred for three minutes. Finally, a certain proportion of EP is added and stirred slowly to obtain the third layer of sample T5#. The second layer is poured onto the third layer when the third-layer composites reached initial setting status. The first layer is prepared in the same way as the second layer. The RL of prepared sample (T5#) is tested from 1.1 GHz to 18 GHz in anechoic chamber using the arched reflection testing method (in Figure **10**(**a**)), according to the Chinese national standard of GJB 2038A-2011. The curves in Figure **10**(**b**) prove that the experimental result comparatively match the calculation result and the reflection loss peak almost disappears. It can be inferred that the EM loss is mainly caused by the absorption of the lossy medium. Destructive interference may exist, but it is weak at each frequency point. The average RL of experimental result is -8.33 dB, and the minimum RL is -10.26 dB at 6.94 GHz. The EAB (RL<-7 dB) is 16.06 GHz, which exhibits an excellent broadband absorption performance. There are some errors between the experimental results and the calculation results, and the possible experimental errors of the composite material were analyzed as follows. There are certain manufacturing accuracy errors when preparing the multilayer cement-based absorbing material. The sample size is 180 mm×180 mm, and there is a strong edge effect in the arch test process. In addition, there are also accuracy errors when testing EM parameters. Therefore, when these aspects of the error are ignored, the wave absorbing performance results of the optimized structure can be considered credible.

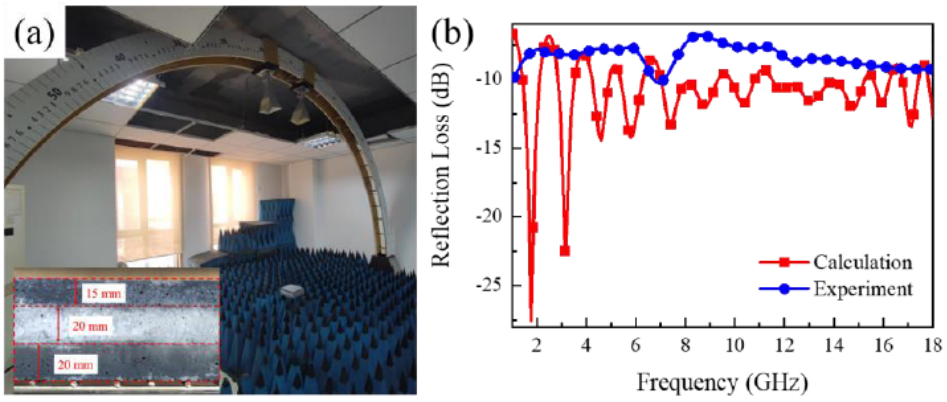

Figure 10: Test process of sample T5# (**a**) and comparison of experiment and calculation result (**b**).

4. CONCLUSION

This paper investigates the use of an optimization with a genetic algorithm for the design of cement based multilayer wave-absorbing composites. A database of EM parameters was thereafter built up through coaxial testing and Boltzmann mixing theory, and the objective function is maximum RL, which can achieve the automatic design of wave absorbing materials, saving experimental time and material costs. The RL of optimal double layer sample D2#, with a thickness of 37.5 mm, is less than -5.96 dB in the full frequency band, with a minimum value of -31.69 dB and an average value of -11.02 dB. The RL of all optimized three layer sample is below –6.89 dB in the full frequency band and the minimum RL of –26.21 dB appears in sample T3#. The experimental result comparatively matches the calculation result, and the reflection loss peak almost disappears. In addition, the optimized result indicates that the intrinsic impedance of first layer is close to that of air, which provides an excellent impedance matching condition for the entry of EM waves. However, the other layers may not meet the impedance gradient principle but still exhibits better EM wave absorption performance. Thus, the application of computer aided technology greatly reduces the difficulty of designing wave-absorbing mortar and can simplify complex EM design problems.

CREDIT AUTHORSHIP CONTRIBUTION STATEMENT

Chao Ma: Conceptualization, Methodology, Validation, Formal analysis, Investigation, Writing - Original Draft, Data curation, Writing - Review & Editing. **Zihao Wu**: Investigation, Methodology. **Shuai Xie**: Resources, Writing - Review & Editing, Supervision, Funding acquisition, Conceptualization, Project administration. **Xin Yang**: Investigation. **Tiantian Si**: Investigation, Visualization. **Junyu Wu**: Investigation. **Zhijiang Ji**: Resources, Methodology, Writing - Review & Editing, Supervision, Funding acquisition, Conceptualization, Project administration. **Jing Wang**: Supervision, Conceptualization. **Chunhong Guo**: Investigation.

CONFLICT OF INTEREST

The authors declare that they have no known competing financial interests or personal relationships that could have appeared to influence the work reported in this paper.

ACKNOWLEDGEMENTS

The authors would like to acknowledge the financial support provided by the Pre-research and Exploration Projects of State Key Laboratory of Green Building Materials (ZA-79).

REFERENCES

[1] Micheli D, Vricella A, Pastore R, *et al*. Synthesis and electromagnetic characterization of frequency selective radar absorbing materials using carbon nanopowders. Carbon 2014; 77: 756-74. https://doi.org/10.1016/j.carbon.2014.05.080

[2] Hou W, Liao Q, Wu M, *et al*. High-performance pinecone-like MOF derivative electromagnetic wave-absorbing composite via in situ anisotropic-oriented growth. J Alloy. Compd. 2023; 937: 168283. https://doi.org/10.1016/j.jallcom.2022.168283

[3] Elmas O. Effects of electromagnetic field exposure on the heart:a systematic review. Toxicol. Ind. Health 2016; 32: 76-82. https://doi.org/10.1177/0748233713498444

[4] Sharma A, Kumar R, Gupta A, *et al*. Enhanced electromagnetic interference shielding properties of phenolic resin derived lightweight carbon foam decorated with electrospun zinc oxide nanofibers. Mater. Today. Commun. 2022; 30: 103055. https://doi.org/10.1016/j.mtcomm.2021.103055

[5] Shu R, Xu J, Wan Z, *et al*. Synthesis of hierarchical porous nitrogen-doped reduced graphene oxide/zinc ferrite composite foams as ultrathin and broadband microwave absorbers. J Colloid Interf. Sci. 2022; 608: 2994-3003. https://doi.org/10.1016/j.jcis.2021.11.030

[6] Stefaniuk D, Sobótka M, Jarczewska K, *et al*. Microstructure properties of cementitious mortars with selected additives for electromagnetic waves absorbing applications. Cem. Concr. Compos. 2022; 104732. https://doi.org/10.1016/j.cemconcomp.2022.104732

[7] Li Z, Hou X, Ke Y, *et al*. Topology optimization with a genetic algorithm for the structural design of composite porous acoustic materials. Appl. Acoust. 2022; 197: 108917. https://doi.org/10.1016/j.apacoust.2022.108917

[8] Guan Z-J, Li R, Jiang J-T, *et al*. Data mining and design of electromagnetic properties of Co/FeSi filled coatings based on genetic algorithms optimized artificial neural networks (GA-ANN). Compos. Part B: Eng. 2021; 226: 109383. https://doi.org/10.1016/j.compositesb.2021.109383

[9] Jang M-S, Jang W-H, Jin D-H, *et al*. Circuit-analog radar absorbing structures using a periodic pattern etched on Ni-coated glass fabric. Compos. Struct. 2022; 281: 115099. https://doi.org/10.1016/j.compstruct.2021.115099

[10] Chamaani S, Mirtaheri SA, Shooredeli MA. Design of very thin wide band absorbers using modified local best particle swarm optimization. AEU - Int. J. Electron. C. 2008; 62: 549-56. https://doi.org/10.1016/j.aeue.2007.06.001

[11] Qi H, Wang DL, Wang SG, *et al*. Inverse transient radiation analysis in one-dimensional non-homogeneous participating slabs using particle swarm optimization algorithms. J Quant. Spectrosc. Ra. 2011; 112: 2507-19. https://doi.org/10.1016/j.jqsrt.2011.06.013

[12] Micheli D, Pastore R, Gradoni G, *et al*. Reduction of satellite electromagnetic scattering by carbon nanostructured multilayers. Acta Astronaut. 2013; 88: 61-73. https://doi.org/10.1016/j.actaastro.2013.03.003

[13] Cheraghi A, Malekfar R, Moemen Bellah S, *et al*. ISO-MANM: An imitation based optimization tool for multilayer microwave absorbers. J Mol. Graph. Model. 2017; 72: 16-24. https://doi.org/10.1016/j.jmgm.2016.11.015

[14] Micheli D, Apollo C, Pastore R, *et al*., Electromagnetic Characterization of Composite Materials and Microwave

Absorbing Modeling. 2011.
https://doi.org/10.5772/15215

[15] Yildizel SA, Toktas A. ABC algorithm-based optimization and evaluation of nano carbon black added multi-layer microwave absorbing ultra weight foam concrete. Mater. Today. Commun. 2022; 32: 104035.
https://doi.org/10.1016/j.mtcomm.2022.104035

[16] Micheli D, Apollo C, Pastore R, *et al*. Nanostructured composite materials for electromagnetic interference shielding applications. Acta Astronaut. 2011; 69: 747-57.
https://doi.org/10.1016/j.actaastro.2011.06.004

[17] Kasgoz A, Korkmaz M, Durmus A. Compositional and structural design of thermoplastic polyurethane/carbon based single and multi-layer composite sheets for high-performance X-band microwave absorbing applications. Polymer 2019; 180: 121672.
https://doi.org/10.1016/j.polymer.2019.121672

[18] Salayong K, Lertwiriyaprapa T, Torrungrueng D, *et al*. Electromagnetic wave absorbing properties of carbon black-filled natural rubber latex. Mater. Today: Proceedings 2022; 52: 2444-8.
https://doi.org/10.1016/j.matpr.2021.10.425

[19] Cao M, Zhu J, Yuan J, *et al*. Computation design and performance prediction towards a multi-layer microwave absorber. Mater. Design. 2002; 23: 557-64.
https://doi.org/10.1016/S0261-3069(02)00023-7

[20] Choi J, Jung H-T. A new triple-layered composite for high-performance broadband microwave absorption. Compos. Struct. 2015; 122: 166-71.
https://doi.org/10.1016/j.compstruct.2014.11.020

[21] Zhang X, Sun W. Three-layer microwave absorber using cement-based composites. Mag. Concr. Res. 2011; 63: 157-62.
https://doi.org/10.1680/macr.9.00196

[22] Eun S-W, Choi W-H, Jang H-K, *et al*. Effect of delamination on the electromagnetic wave absorbing performance of radar absorbing structures. Compos. Sci. Technol. 2015; 116: 18-25.
https://doi.org/10.1016/j.compscitech.2015.04.001

[23] Wang Z, Wang Z, Ning M. Optimization of electromagnetic wave absorption bandwidth of cement-based composites with doped expanded perlite. Constr. Build. Mater. 2020; 259: 119863.
https://doi.org/10.1016/j.conbuildmat.2020.119863

[24] Jang D, Choi BH, Yoon HN, *et al*. Improved electromagnetic wave shielding capability of carbonyl iron powder-embedded lightweight CFRP composites. Compos. Struct. 2022; 286: 115326.
https://doi.org/10.1016/j.compstruct.2022.115326

[25] Negi P, Gupta A, Singh M, *et al*. Excellent microwave absorbing and electromagnetic shielding performance of grown MWCNT on activated carbon bifunctional composite. Carbon 2022; 198: 151-61.
https://doi.org/10.1016/j.carbon.2022.07.024

[26] Wang H, Zhang Y, Wang Q, *et al*. Biomass carbon derived from pine nut shells decorated with NiO nanoflakes for enhanced microwave absorption properties. RSC Advances 2019; 9: 9126-35.
https://doi.org/10.1039/C9RA00466A

[27] Ciuchi IV, Olariu CS, Mitoseriu L. Determination of bone mineral volume fraction using impedance analysis and Bruggeman model. Mater. Sci. Eng. 2013; 178: 1296-302.
https://doi.org/10.1016/j.mseb.2013.04.001

[28] Zhai Y, Zhang Y, Ren W. Electromagnetic characteristic and microwave absorbing performance of different carbon-based hydrogenated acrylonitrile-butadiene rubber composites. Mater. Chem. Phys. 2012; 133: 176-81.
https://doi.org/10.1016/j.matchemphys.2012.01.004

[29] Guihard V, Patapy C, Sanahuja J, *et al*. Effective medium theories in electromagnetism for the prediction of water content in cement pastes. Int. J. Eng. Sci. 2020; 150: 103273.
https://doi.org/10.1016/j.ijengsci.2020.103273

[30] Sihvola AH, Alanen E. Studies of mixing formulae in the complex plane. IEEE T. Geosci. Remote. 1991; 29: 679-87.
https://doi.org/10.1109/36.135831

[31] Xia L, Feng Y, Zhao B. Intrinsic mechanism and multiphysics analysis of electromagnetic wave absorbing materials: New horizons and breakthrough. J. Magn. Magn. Mater. 2022; 130: 136-56.
https://doi.org/10.1016/j.jmst.2022.05.010

[32] Guan Z-J, Jiang J-T, Yan S-J, *et al*. Sandwich-like cobalt/reduced graphene oxide/cobalt composite structure presenting synergetic electromagnetic loss effect. J Colloid Interf. Sci. 2020; 561: 687-95.
https://doi.org/10.1016/j.jcis.2019.11.045

[33] Zhang X, Sun W. Microwave absorbing properties of double-layer cementitious composites containing Mn-Zn ferrite. Cem. Concr. Compos. 2010; 32: 726-30.
https://doi.org/10.1016/j.cemconcomp.2010.07.013

[34] Misra PK, Chapter 12 - Diamagnetism and Paramagnetism. in: Misra PK (Ed)Phys. Condens. Matter.Academic Press, Boston, 2012, pp. 369-407.
https://doi.org/10.1016/B978-0-12-384954-0.00012-8

[35] Xie S, Ma C, Ji Z, *et al*. Electromagnetic wave absorption and heat storage dual-functional cement composites incorporated with carbon nanotubes and phase change microcapsule. J Build. Eng. 2023; 67: 105925.
https://doi.org/10.1016/j.jobe.2023.105925

[36] Liu J, Wang G, Liu C, *et al*. Novel lightweight and efficient electromagnetic waves absorbing performance of biomass porous carbon/polymer-derived composite ceramics. Ceramics International 2023; 49: 13742-51.
https://doi.org/10.1016/j.ceramint.2022.12.252

[37] Zhang H, Ji H, Dai G, *et al*. Nanoarchitectonics of integrated impedance gradient MXene/PPy/polyester composite fabric for enhanced microwave absorption performances. Compos. Part A: Appl. S. 2022; 163: 107163.
https://doi.org/10.1016/j.compositesa.2022.107163

[38] Pan J, Li X, Xia W, *et al*. Improveament of multiple attenuation and optimized impedance gradient for excellent multilayer microwave absorbers derived from two-dimensional metal-organic frameworks. Chem. Eng. J 2023; 452: 139601.
https://doi.org/10.1016/j.cej.2022.139601

Received on 12-04-2023 Accepted on 02-05-2023 Published on 04-05-2023

DOI: https://doi.org/10.31875/2410-4701.2023.10.04